HAL
open science

Gas transfer experiment on a lake (Kerguelen Islands) using 3 He and SF 6

Philippe Jean-Baptiste, Alain Poisson

To cite this version:

Philippe Jean-Baptiste, Alain Poisson. Gas transfer experiment on a lake (Kerguelen Islands) using 3 He and SF 6. Journal of Geophysical Research. Oceans, 2000, 105 (C1), pp.1177-1186. 10.1029/1999JC900088 . hal-03122972

HAL Id: hal-03122972

https://hal.science/hal-03122972v1

Submitted on 27 Jan 2021

HAL is a multi-disciplinary open access archive for the deposit and dissemination of scientific research documents, whether they are published or not. The documents may come from teaching and research institutions in France or abroad, or from public or private research centers.

L'archive ouverte pluridisciplinaire **HAL**, est destinée au dépôt et à la diffusion de documents scientifiques de niveau recherche, publiés ou non, émanant des établissements d'enseignement et de recherche français ou étrangers, des laboratoires publics ou privés.

JOURNAL OF GEOPHYSICAL RESEARCH, VOL. 105, NO. C1, PAGES 1177–1186, JANUARY 15, 2000

Gas transfer experiment on a lake (Kerguelen Islands) using ^{3}He and SF_6

Philippe Jean-Baptiste
Laboratoire des Sciences du Climat et de l'Environnement, CEA/CNRS, Centre d'études de Saclay, Gif/Yvette, France

Alain Poisson
Laboratoire de Physique et Chimie Marines, CNRS/UPMC, Paris

Abstract. Gas transfer velocities of SF_6 and ^{3}He were determined in a Kerguelen Islands lake at wind speeds in the range 0-10 m/s by injecting the two tracers into the water and measuring their concentrations over 40 days. Two methods are investigated for the determination of the relationship linking the gas transfer velocity K to the wind speed W. The first method postulates a power law relationship $K=\beta W^{\alpha}$. This leads to the same exponent $\alpha=1.5\pm0.2$ for both gases. The second method is the classic determination of the gas transfer velocity K_{ij} between two tracer measurements at times t_i and t_j using the well-mixed reservoir assumption. This method proves to be less favorable owing to its nonlinearity bias and also because it induces much scatter in the gas transfer coefficient/wind speed relationship. This dispersion is shown to arise from the experimental scatter of the data and, above all, from the high sensitivity of the method to even small heterogeneities in the tracer vertical distribution. In the present experiment, the Liss and Merlivat correlation [*Liss and Merlivat, 1986*] is shown to underestimate the actual mean gas exchange rate by about 40% Our results agree with the recent dual-tracer experiment by *Wanninkhof et al.* [1993] and are also consistent with CO_2 transfer coefficient data derived from the study of ^{14}C oceanic inventories. As expected from gas transfer theories and various experimental observations, the Schmidt number exponent in the comparison of ^{3}He and SF_6 transfer velocities is found to vary substantially with the transfer regime. However, its variation is found to be greater than that forecast by current gas transfer models, with values as high as n=-0.2 for intermediate to strong winds. This again raises the question of the validity of the normalization method for K_{CO2} calculation from gas transfer experiments, especially in high-wind regimes.

1. Introduction

The process of air/water exchange of gases is particularly important for our understanding of the biogeochemical cycle of environmentally active gases such as CO_2, CH_4, N_2O, dimethylsulfide, chlorofluorocarbons, etc. Most efforts have been directed toward defining a reliable relationship between the transfer velocity K and the wind speed W, a key parameter in gas transfer dynamics, which determines, to a large extent, the dynamic state of the air-sea boundary and the physics of gas exchange. Numerous studies have been made under various conditions including laboratory, wind tunnels of different sizes, and field experiments in lakes or the open- sea. Results from the field studies are shown in Figure 1. Three distinct wave formation regions have been identified, which correspond to changes in the slope of the correlation between K and W [*Liss and Merlivat*, 1986]. In the first region (W <2-3 m/s), K increases only slightly with the wind speed. The second region corresponds to the occurrence of capillary waves (2-3 m/s <W <10-13 m/s), with an increased dependence of K on W. The third region, which shows the greatest change in K with increased wind speed, is characterized by the occurrence of breaking waves and additional gas exchange through bubbles. In spite of intense efforts in determining the functional form of the transfer velocity–wind speed relationship, the results still show large uncertainties (see references in Figure 1). Most results are bracketed by the empirical relation proposed by *Liss and Merlivat* [1986] on the lower side and by that of *Smethie et al.* [1985] on the higher side, with no clear tendency regarding the type of experiments (laboratory, lake, or open sea) or the kind of tracer studied. In fact, we must not expect to find a strictly unique relationship, because the wind speed remains a "phenomenological" parameter that can describe only approximately the real physical and dynamic conditions at the interface. This fact is undoubtedly one significant cause for the large scatter among the various results reported in the literature.

Nevertheless, for practical purposes, good knowledge of the transfer velocity–wind speed correlation is of great importance for computing fluxes at a global scale and for modeling global biogeochemical cycles. With respect to the specific carbon cycle problem, aimed at assessing the fate of anthropogenic CO_2 emissions, very useful data for evaluating the CO_2 transfer coefficient have been obtained directly from the study of natural and bomb $^{14}CO_2$ transfer between the atmosphere and the ocean [*Broecker et al.*, 1980, 1985; *Cember*, 1989]. However, most measurements published to date were carried out with different gases (Rn, SF_6, ^{3}He) and then adapted to CO_2 using the theoretical relationship (1) that links the transfer coefficients of two gases K_i and K_j, to their respective Schmidt numbers Sc_i and Sc_j (the Schmidt number is a dimensionless number defined as the ratio of the kinematic viscosity of water ν to the gas molecular diffusivity D, $Sc=\nu/D$).

Copyright 2000 by the American Geophysical Union.

Paper number 1999JC900088.
0148-0227/00/1999/JC900088$09.00

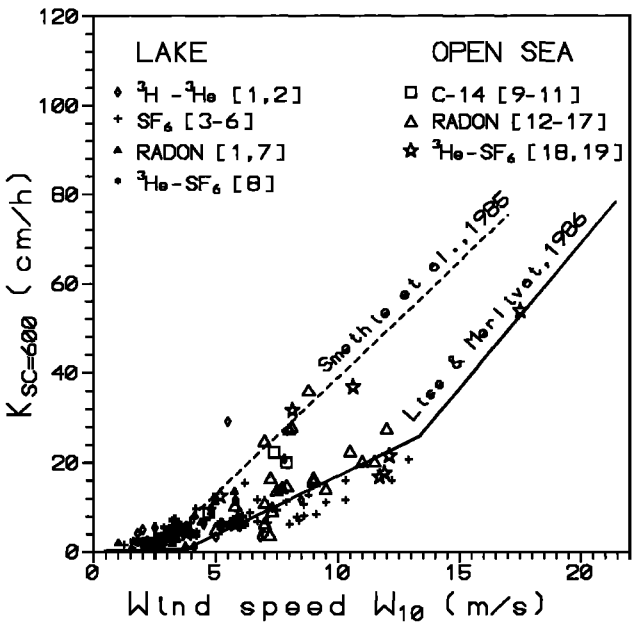

Figure 1. Literature data for gas transfer versus wind speed field experiments (normalized to CO_2 Schmidt number Sc=600). Lake data are from 1, *Torgersen et al.* [1982]; 2, *Jähne et al.* [1984a]; 3, *Wanninkhof et al.* [1985]; 4, *Wanninkhof et al.* [1987]; 5, *Wanninkhof et al.* [1991b]; 6, *Upstill-Goddard et al.* [1990]; 7, *Emerson et al.* [1973], and 8, *Clark et al.* [1995]. Open-sea data are from 9, *Broecker et al.* [1980]; 10, *Broecker et al.* [1985]; 11, *Cember* [1989]; 12, *Broecker and Peng* [1971]; 13, *Peng et al.* [1974]; 14, *Peng et al.* [1979]; 15, *Kromer and Roether* [1983]; 16, *Smethie et al.* [1985]; 17, *Glover and Reeburgh* [1987]; 18, *Watson et al.* [1991]; and 19, *Wanninkhof et al.* [1993].

$$K_i/K_j=(Sc_i/Sc_j)^n \qquad n<0 \qquad (1)$$

The value of the Schmidt number exponent n has been the focus of both theoretical and experimental studies. A review of the different theoretical results is given by *Liss and Merlivat* [1986] and is summarized in Table 1. The differences in the value of n correspond to various assumptions regarding the boundary layer processes and boundary conditions, corresponding to different dynamic states of the interface, going from purely diffusive to turbulent. A number of determinations of this exponent have been carried out in laboratory or field experiments, which are also summarized in Table 1. Both theoretical and experimental approaches agree on the fact that the value of n tends to increase (i.e., become less negative) when the transfer regime becomes more energetic. The various models forecast values rising from -2/3 at low to -1/2 at higher regimes. Experimental values follow the same trend To compare gas transfer velocities in intermediate- and high-wind regimes, they are usually normalized to the Schmidt number of CO_2 at 20°C (Sc=600) with n =-0.5. However, there is no evidence that this value of the Schmidt number exponent is an upper limit and remains constant. On the contrary, experimental data [*Wanninkhof et al.*, 1993] suggest that this value keeps on increasing (i e, becomes less negative) for more turbulent regimes. This situation can lead to a systematic bias in gas transfer determinations, especially for high wind speeds.

To obtain new data on the gas transfer velocity–wind speed relationship and to gather new evidence for the variation of the Schmidt number exponent, we have carried out a dual-tracer experiment in a Kerguelen Islands lake.

2. Experimental Design

The Kerguelen Islands (Figure 2) are in the southern Indian Ocean in the 40-50 S latitude belt, where winds are usually quite strong. Lake Suisse, where the experiment was carried out, is a freshwater lake approximately 1 km wide and 5 km long, with a mean depth of 46.6 m (maximum depth 91m), corresponding to a volume of 0.215 km^3 [*Poisson et al.*, 1990]. Owing to the local topography, the direction of the wind is mainly parallel to the long axis of the lake.

The lake has very steep slopes, so that the potential bias in the determination of any tracer gas transfer coefficient due to shallow parts is minimized. From monitoring the water flow out of the lake, its renewal rate was estimated to be of the order of only 0.8% during the time of the experiment. Hence this term is neglected in the tracers' mass balance. Surface water temperature during the experiment was constant (8°C), and vertical temperature profiles also revealed a constant temperature with depth, with only a 0.09°C difference between the surface and bottom layers (z = -83 m). This indicates that the lake is thermally homogeneous and nonstratified. In the following, we shall see, however, that, in spite of this, small vertical gradients in the tracer concentrations can develop during strong wind episodes. This fact is generally overlooked in most studies, and a fully homogenized tracer distribution is usually assumed. The possible effect of this slight nonhomogeneous tracer distribution will be discussed in section 3.3.

The two tracers (SF_6 and ^3He) were released from two aluminum tanks containing respectively, 3 m^3 of SF_6 and 1 L STP of ^3He mixed with nitrogen to give a total pressure of 150 bar. The tanks were towed in the deep layers of the lake, and the gases were released through a set of diffusing stones over 8 hours. The homogenization of the tracers in the water was then monitored at

Table 1. Theoretical Values of the Schmidt Number Exponent n in Equation (1) and Literature Compilation of the Range of Variation of n for Various Types of Experiments and Transfer Regimes

Schmidt Number Exponent n	References
	Models
-1[a]	*Whitman* [1923]
-2/3[b]	*Deacon* [1977]
-0.5[c]	*Higbie* [1935]
	Laboratory Experiments
-0.56	*Gilliland and Sherwood* [1934]
-0 31± 0.05	*Hutchinson & Sherwood* [1937]
-0.47	*Sherwood & Holloway* [1940]
-0.58	*Dawson & Trass* [1972]
-0.704	*Shaw & Hanratty* [1977]
-0 41± 0 09	*Jähne et al.* [1979]
-0 55/-0 67	*Jähne et al.* [1984b]
-0.45/-0.50	*Ledwell* [1984]
-0.41/-0.75	*Jähne et al.* [1987b]
-0 30_b/-0 53	*Wanninkhof et al.* [1993]
	Field Experiments
-0.62/-0.75[d]	*Torgersen et al.* [1982]
-0.505/-0.515	*Watson et al.* [1991]
-0.35_b/-0 56	*Wanninkhof et al.* [1993]
-0.57/-0.59	*Clark et al* [1995]
-0.2_b/-0 9	this work

Subscript b indicates a possible contribution of bubbles to the transfer.

[a] Thin film model.

[b] Boundary layer model.

[c] Surface renewal model.

[d] Value was recalculated with Schmidt numbers from *Wanninkhof* [1992]

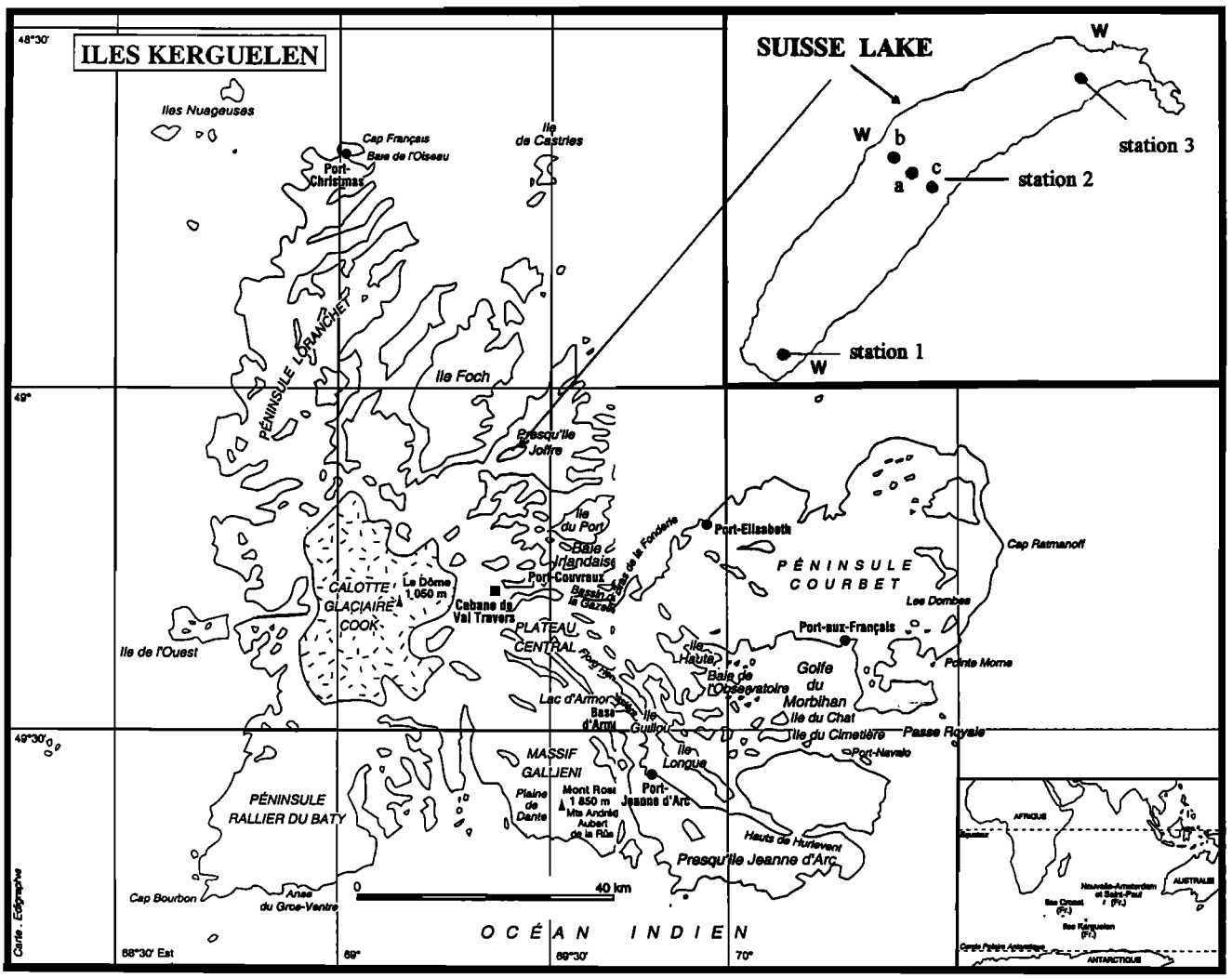

Figure 2. Map of Lake Suisse and the Kerguelen Islands

different positions in the lake by SF_6 measurements using gas chromatography equipment on the shore. After 48 hours, the tracer distribution in the lake could be considered homogeneous and monitoring the escape rate of both gases was started. SF_6 and ^{3}He samples were taken at regular intervals at station 2a located at the center of the lake (Figure 2) using hydrographic bottles. These samples were collected near the surface (z = -1.5 m). SF_6 samples (and some additional ^{3}He samples) were also at stations 2b and 2c (in the middle of the lake) and at stations 1 and 3 at both ends of the lake (Figure 2) to monitor the overall homogeneity of the tracer distribution. Wind speeds were recorded at a height of 4 m at three different positions on the shore (indicated by the letter W in Figure 2). The time-series of the three anemometers are in good agreement, with differences not exceeding 10%. For relating gas transfer to wind speed, raw wind speeds were converted to the standard wind speed W_{10} at 10 m height following *Large and Pond* [1981], leading to a correction factor of around 1.10. SF_6 samples were analyzed in a container laboratory installed on the shore using the same technique as described by *Wanninkhof et al.* [1991a]. Analytical precision was within ±1% (1σ error). Helium samples were taken in copper tubes and returned to the laboratory at Saclay for helium extraction and mass spectrometric measurement using our standard procedure [*Jean-Baptiste et al.*, 1992] for oceanic samples. Note that since the ^{4}He concentration is at its natural background and is essentially constant, the ^{3}He concentrations are expressed as an isotopic ratio R=^{3}He/^{4}He using the delta notation:

$$\delta^3\mathrm{He}(\%) = (R/R_a - 1)\times 100$$

where R_a is the atmospheric helium isotopic ratio. The overall relative uncertainty in the ^{3}He/^{4}He ratio, $\Delta R/R$ is less than 0.5% (1σ error).

3. Tracers Results and Gas Transfer Velocity/Wind Speed Relationship

SF_6 and ^{3}He time-series at station 2a, located at the center of the lake, are displayed in Figure 3 along with the record of the wind speed. Both ^{3}He and SF_6 records show a steady decrease of the tracer concentration due to gas escape to the atmosphere. Over the 30 days of available SF_6 measurements at station 2a, SF_6 concentrations were divided by 3.7. During the same period, ^{3}He concentrations were reduced even more rapidly, by a factor of 6 7, as expected from the greater diffusivity of ^{3}He. The plot of the logarithm of the tracers concentrations versus time (Figure 4) shows that the decay of both tracers is exponential.

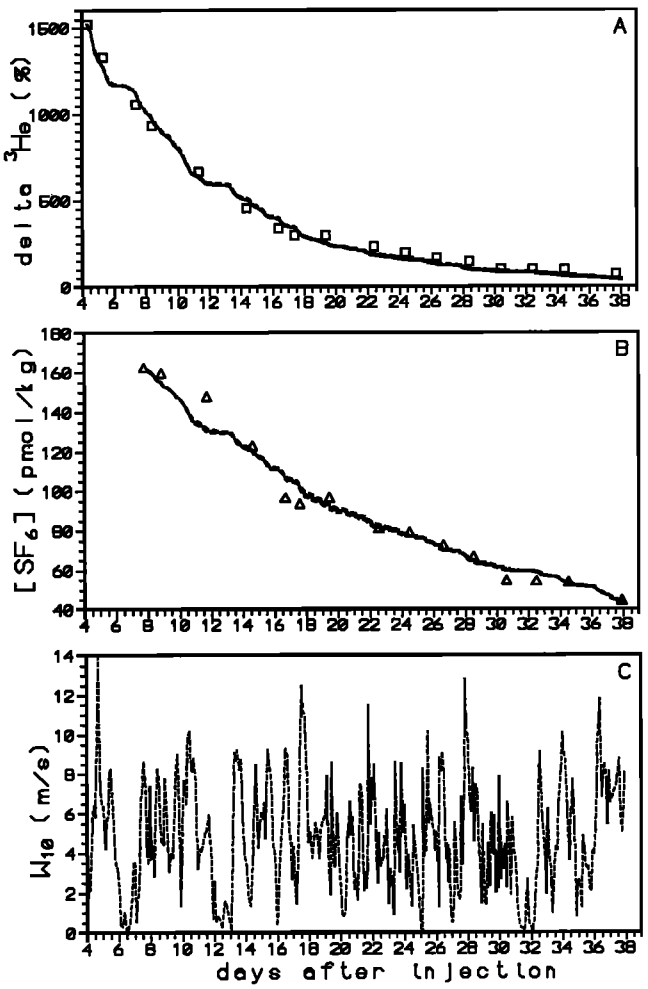

Figure 3. (a) Decline of SF_6 concentration and (b) excess ^{3}He (δ^3He%) with time, (c) mean wind speed corrected to 10 m, W_{10}. The solid line for SF_6 and δ^3He is the best fit of the data using a power law $K=\beta W^{\alpha}$, with $\alpha=1.5$ (see section 3.1), and the dashed lines correspond to $\alpha=1.3$ and 1.7

From these time-series, we calculate the gas transfer velocities versus wind speed in two different ways. First (section 3.1), we assume that this relationship can be well represented by a power law, $K = \beta W^{\alpha}_{10}$, where K is transfer velocity and W_{10} is wind speed at 10 m height, and we fit the parameters α and β to our experimental data. The second method (section 3.2) simply consists of calculating the mean transfer velocity, according to (4), and the mean wind speed for each successive data point.

In the following, both methods are explained, with their respective advantages and limitations, and their results are compared. Then, we look at the potential effect of even slight vertical heterogeneities in the tracers' concentrations on the determination of the gas transfer velocities.

3.1. Determination of a Functional Form $K = \beta W^{\alpha}$

For the sake of simplicity, we first assume that the gas transfer velocity versus wind speed relationship can be represented by a power law, $K = \beta W^{\alpha}$. This choice seems reasonable to us in light of the available data in the literature, which indeed display this type of behavior. Moreover, this method avoids the problem of the nonlinearity bias that arises when calculating mean transfer velocities versus mean wind speeds, as we shall see in section 3.2 when using the second method. For each tracer, the α and β coefficients are adjusted by solving the tracer mass balance equation (equations (2a) and (2b) for SF_6 and ^{3}He, respectively) for the lake between time t and $t+dt$, with surface tracer fluxes Φ forced by the measured wind speed (see (3a) and (3b)), so as to minimize the mismatch between the calculated δ^3He(t) and $C_{SF6}(t)$ curves and the data. This mismatch is defined as the squared distance between the measured concentrations and the calculated curve.

$$C_{SF6}(t+dt) = C_{SF6}(t) - \Phi_{SF6}(t)\times dt/h \quad (2a)$$

$$\delta^3\mathrm{He}(t+dt) = \delta^3\mathrm{He}(t) - \Phi_{3He}(t)\times dt/h \quad (2b)$$

where h is mean depth and with

$$\Phi_{SF6}(t) = \beta_{SF6} W^{\alpha_{SF6}} [C_{SF6}(t) - C_{eq}] \quad (3a)$$

with $C_{eq} = 0$.

$$\Phi_{3He}(t) = \beta_{3He} W^{\alpha_{3He}} [\delta^3\mathrm{He}(t) - \delta_{eq}] \quad (3b)$$

with $\delta_{eq} = -1.6\%$ [*Weiss*, 1970; *Top et al.*, 1987].

In the applicable range of wind speeds (0-10 m/s), this best fit procedure leads to $\alpha \approx 1.5$ for both gases, β_{SF6}=0.71±0.06 and β_{3He}=1 8±0.1 (for K in cm/h and W_{10} in m/s). The quality of the fit is only a weak function of the exponent α in the range 1.3-1.7 as shown in Figure 3 where the dashed lines, representing the best fit curves for α =1.3 and 1.7, are almost indistinguishable from the solid curve (corresponding to α =1.5). This value $\alpha \approx 1.5\pm0.2$ compares well with the 1.64 exponent value derived by *Wanninkhof et al.* (1991b] from a lake experiment using SF_6.

Our results correspond to a mean Schmidt number exponent of -0 43±0.1 for the complete experiment, with Schmidt numbers for ^{3}He and SF_6 of 219 and 1912, respectively [*Jähne et al.*, 1987a; *King and Saltzman*, 1995]. In Figure 5, the gas transfer velocity/wind speed relationships for both tracers are normalized to CO_2 at 20°C (Sc=600) using a Schmidt number exponent n=-0 5, as is usually done in the literature for comparison purposes.

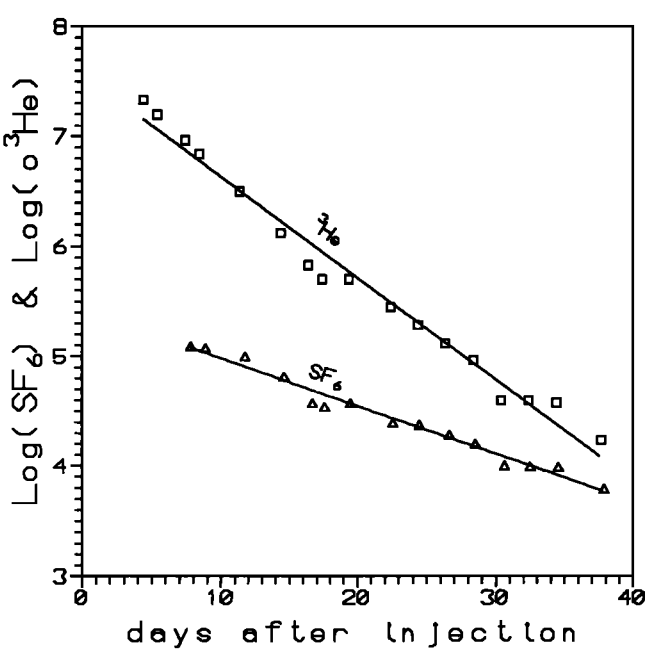

Figure 4. Logarithm of the tracers' concentrations (SF_6 and δ^3He%) versus time

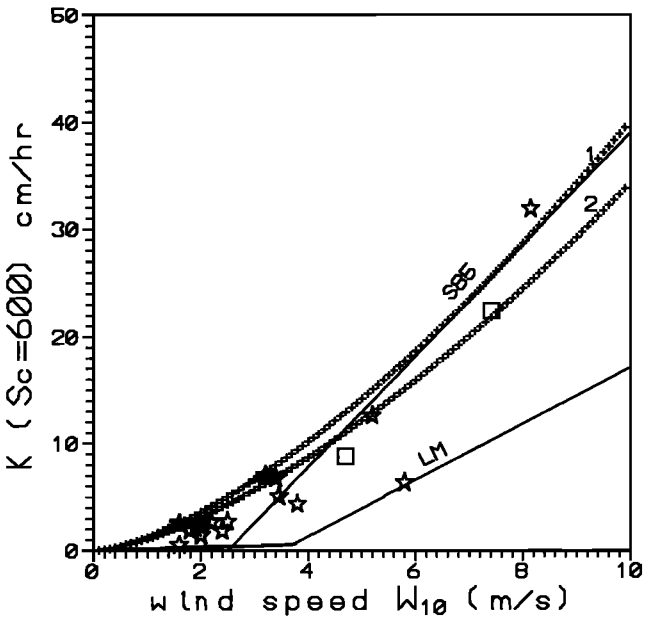

Figure 5. Transfer velocity, normalized to CO_2 (Sc=600) using a constant Schmidt number exponent n=-0.5, plotted against wind speed W_{10}. Curves labeled 1 and 2 are the present results for SF_6 and ^{3}He, respectively. LM and S85 stand for the *Liss and Merlivat* [1986] and *Smethie et al.* [1985] relationships, respectively. The two open squares are global ^{14}C transfer coefficients from *Broecker et al.* [1985] and *Cember* [1989]. The solid stars are the dual-tracer results of *Watson et al.* [1991] and the open stars are from *Wanninkhof et al.* [1993] and *Clark et al.* [1995].

In the Lake Suisse experiment, the curves deduced from ^{3}He and SF_6 significantly disagree with those from *Liss and Merlivat* [1986]. To show the practical consequences of this large mismatch, we display the δ^3He time -series that would result from the *Liss and Merlivat* [1986] (LM) relationship (applied to ^{3}He using the exponent n =-0.5) in Figure 6. The LM relationship underestimates the ^{3}He mean evasion rate actually deduced from the present experiment by 40% (a figure that corresponds to the factor that must be applied to the ^{3}He transfer coefficient K_{3He}=1.8×W$^{1.5}$ to fit the curve calculated with the LM correlation in Figure 6).

Our results are on the higher side of the literature data. They are consistent with the gas transfer velocities derived from ^{14}C

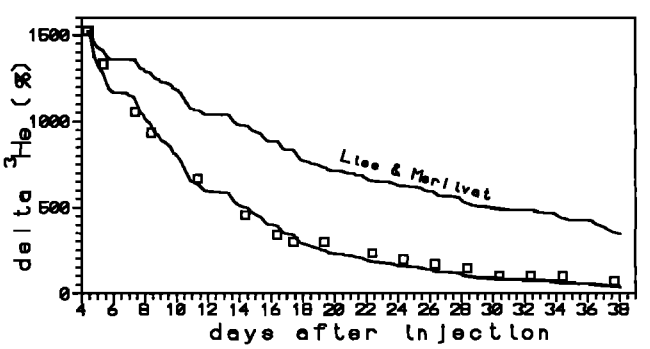

Figure 6. Computed δ^3He time -series that would result from the use of the *Liss and Merlivat* [1986] relationship (solid line) and comparison with the measured δ^3He (squares).

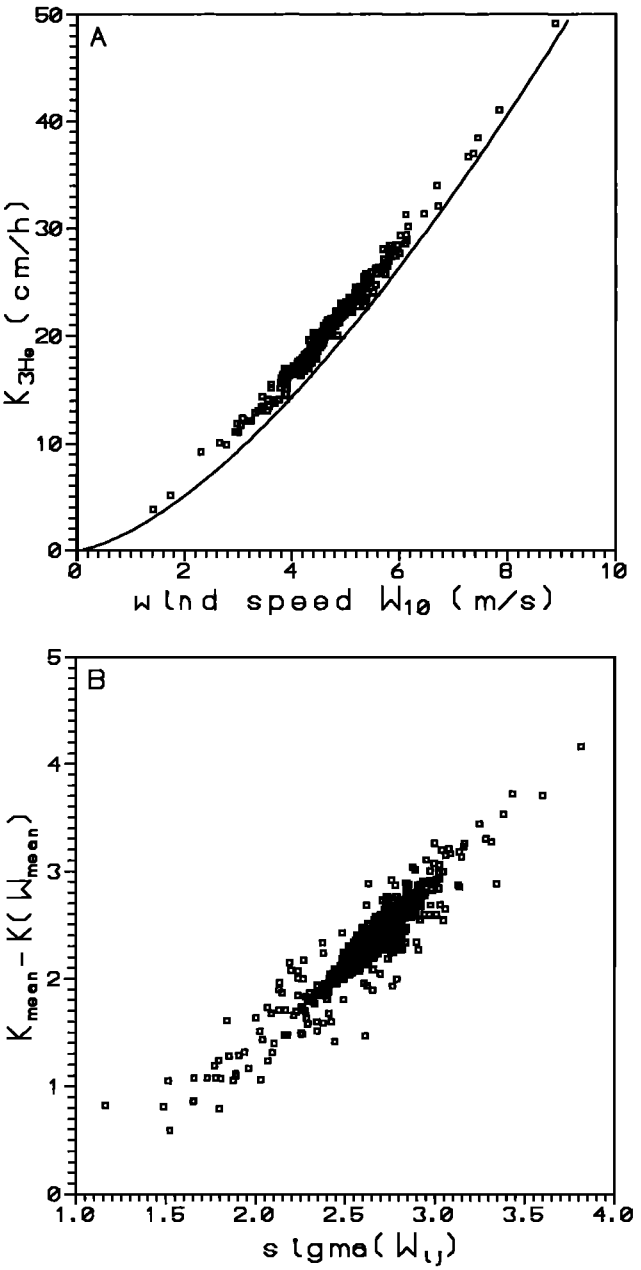

Figure 7. (a) Comparison, for ^{3}He, between the K_{ij}-W_{ij} couples (open squares) calculated from equation (4) and the power law K_{3He}=1.8×$W^{1.5}$ determined in section 3 1. The (i,j) couples used for calculating K_{ij} were selected along the δ^3He(t) best fit curve computed from (2b) and (3b) (well-mixed box model) using the law K_{3He}=1.8×$W^{1.5}$. The difference between the solid curve (representing K=1.8×$W^{1.5}$) and the open squares is due to the non-linearity bias. (b) Bias shown as an increasing function of the wind speed variability, expressed as the sigma of the wind speed distribution (σ_{ij}) between times t_i and t_j .

oceanic inventories, which appear to be among the most robust field determinations because they represent global long-term averages. They are also in good agreement with the results of *Wanninkhof et al.* [1993] obtained with the same tracer pair (^{3}He and SF_6) on Georges Bank. For low wind speeds, the present results tend to be slightly above *Clark et al.*'s [1995] recent ^{3}He-SF_6 data (Figure 5).

3.2. Individual K_{ij} Determinations

For each gas, a mean transfer velocity K_{ij} and a mean wind speed W_{ij} can be computed for two successive measurements at times t_i and t_j respectively, by the standard equation:

$$K_{ij}=h/(t_j-t_i)\ [\ln (C_i-C_{eq})/(C_j-C_{eq})] \quad (4)$$

where C_i and C_j are the measured concentrations (for SF_6) and the measured δ^3He(%) (for helium) at times t_i and t_j, respectively, and h is the mean depth of the lake (h=46.6 m). The suscript "eq" denotes the tracer background at equilibrium with the atmosphere: C_{eq}=0 for SF_6 and $\delta^3He_{eq} \approx$ -1.6% [*Weiss*, 1970; *Top et al.*, 1987]. In fact, there is no theoretical reason to restrict this calculation to consecutive data points only, and the method can be extended to every possible pair of measurements C_i and C_j at times t_i and t_j, with K_{ij} being the mean transfer velocity averaged over the time period t_j-t_i and W_{ij} the mean wind speed over the same period. The main drawback of this method is the bias in the determination of the transfer velocity/wind speed relationship owing to its nonlinear nature; that is, K_{ij} does not equal $K(W_{ij})$. This bias is clearly noticeable on the example displayed in Figure 7a; here the squares represent all the K_{ij} versus W_{ij} pairs determined from fictive δ^3He data points selected at a 1-day frequency on the theoretical curve δ^3He(t) of section 3.1 computed using the power law K(cm/h)=1.8×$W^{1.5}$. The solid curve is the power law K(cm/h)=1.8×$W^{1.5}$. If there was no bias, the points would lie exactly on the curve. Figure 7b shows that, as expected, the bias is indeed a growing function of the sigma of the wind speed distribution (σ_{ij}) between time t_i and t_j, with bias up to 20% for episodes of higher wind variability.

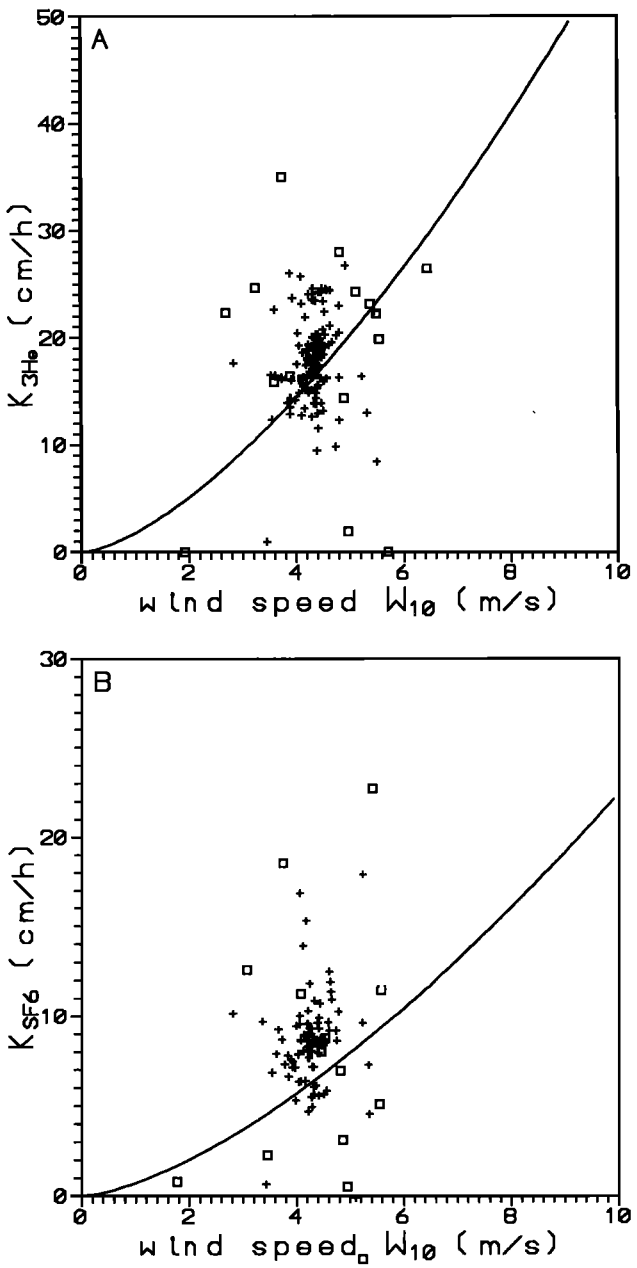

Figure 8. Calculated K values versus mean wind speed for every possible pair of (a) δ^3He and (b) SF_6 measurements. (The few negative values of K, due to some negative values of the tracer concentration difference C_i-C_j , were eliminated because they are physically meaningless.) Open squares denote K values calculated from adjacent data points. For each tracer, the power law K = βW^{α}_{10} determined using method 1 is included for comparison.

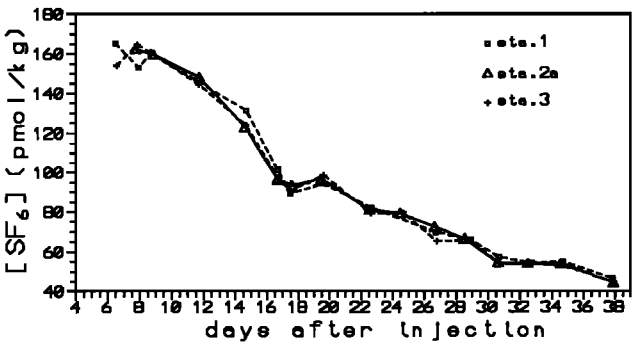

Figure 9. Comparison of SF_6 surface concentrations measured at stations 1, 2a, and 3.

Figures 8a and 8b display all possible K_{ij} versus mean wind speed W_{ij} pairs deduced from our ^{3}He and SF_6 measurements (the open squares denote K_{ij} corresponding to successive measurements) and compare the results to the functional forms K = $\beta W^{1.5}$ obtained in section 3.1. In addition to the nonlinearity bias discussed above, this second method clearly leads to a large scatter in the K_{ij} determinations (note that this scatter is not reduced when selecting only successive measurements). For these two reasons, we favor the first approach (method 1) which avoids the nonlinearity problem and smooths out the experimental scatter. In the following section, we examine the possible effects of small heterogeneities in the vertical distribution of the tracers and show that much of the scatter in the K_{ij} determination is indeed related to these heterogeneities.

3.3. Heterogeneity Effects

Almost all of the studies published to-date assume a well-mixed reservoir. Vertical mixing is assumed to be efficient enough to ensure a homogeneous vertical tracer distribution. Possible horizontal heterogeneities effects due, for instance, to the occurrence of shallow parts, are also ignored. In the present experiment, unlike δ^3He measurements which were mostly made in the surface layer at one central station, a number of SF_6 samples were taken at different depths at every station indicated in Figure 2 to monitor the degree of homogeneity of the lake. This monitoring shows (Figure 9) that there is no horizontal tracer gradient. However, the SF_6 water column profiles show

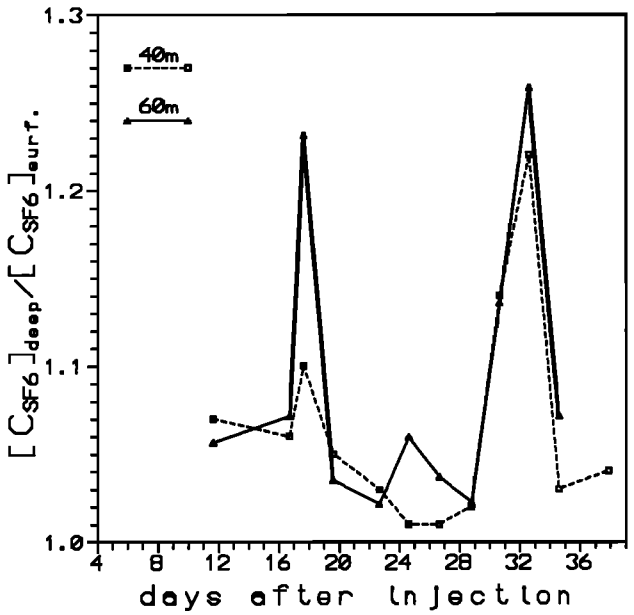

Figure 10. Time -series at station 2a of the ratio between measured SF_6 concentrations at lake deep waters (at depths z=-60 and -40 m) and at surface waters.

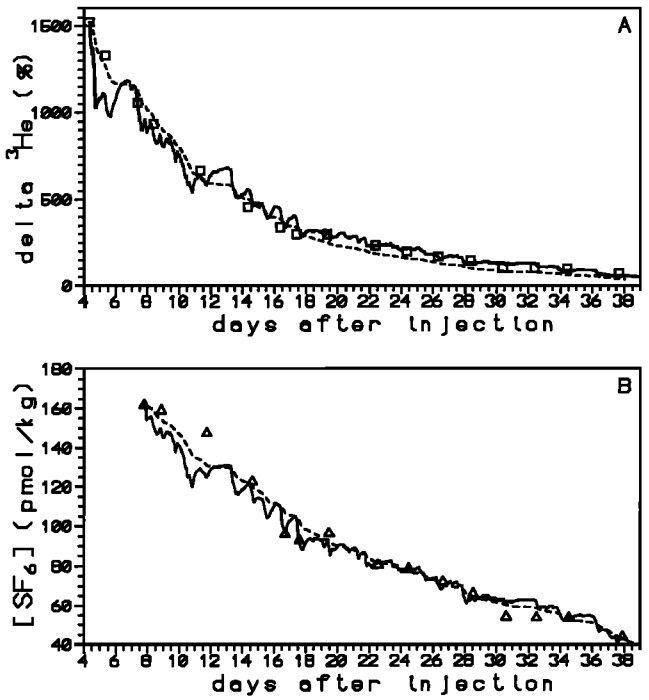

Figure 11. Best fit curve (solid line) of the (a) δ^3He and (b) SF_6 measured surface concentration time -series using the vertical diffusion model. The dashed line is the best fit curve with the well-mixed box model (see Figure 3) and is included here for comparison.

that SF_6 concentrations in the deep layers sometimes tend to be significantly higher than surface concentrations (Figure 10), hence leading to some heterogeneity in the tracer vertical distribution. This means that although the convective mixing of the lake is rapid owing to the lack of stratification, it is not instantaneous. Hence it takes some time for the surface layer to be resupplied with the tracers from deeper layers, especially during high wind episodes. In the following, we look at the consequences of this phenomenon on the determination of the gas transfer velocity. Instead of assuming a well-mixed reservoir, we consider a vertical diffusivity D_v of the tracer in water. The vertical distribution of SF_6 versus time is computed using a 20-layer diffusion model developed for this study. At each time step, the tracer fluxes exchanged between each layer (with a constant thickness $dz=h/20$) and its neighbors are computed using Fick's law (equations 5a and 5b) and the tracer concentration in each layer is then computed from the mass balance equation (6).

$$F_{i,i+1}(t) = -D_v[C_i(t) - C_{i+1}(t)]/dz \qquad (5a)$$

where $F_{i,i+1}(t)$ is the flux between layer i and i+1, with

$$F_{\text{bottom}} = 0, F_{\text{surf}} = \beta W^{1.5}[C_1(t) - C_{eq}] \qquad (5b)$$

$$C_i(t+dt) = C_i(t) + dt/dz\,[F_{i,i+1}(t) - F_{i,i-1}(t)] \qquad (6)$$

In addition to the parameters α and β, which are adjusted as in section 3.1 to minimize the mismatch between the experimental data and the calculated $SF_6(t)$ curve for the surface layer, the diffusivity D_v is also tuned simultaneously so as to reproduce the range of observed vertical concentration gradients between surface and deep SF_6 concentrations shown in Figure 10. Our best estimate of the vertical diffusion coefficient is $D_v \approx 50$ cm^2/s. This value is on the higher side of vertical diffusivities observed in nature [*Broecker and Peng*, 1982], which is consistent with a nonstratified lake. Although the computed time evolution of the surface concentration is more "wavy" (Figure 11), as expected from a physical point of view, the coefficients of the power law $K_{SF6} = \beta W^{\alpha}$ remain basically unchanged, thereby fully justifying the homogeneity assumption used in method 1.

However, if method 2 is used, the consequences are important: Figure 12 is identical to Figure 7a, but this time the theoretical curve δ^3He(t) is the concentration in the surface layer of the 20-layer diffusion model instead of the concentration calculated with

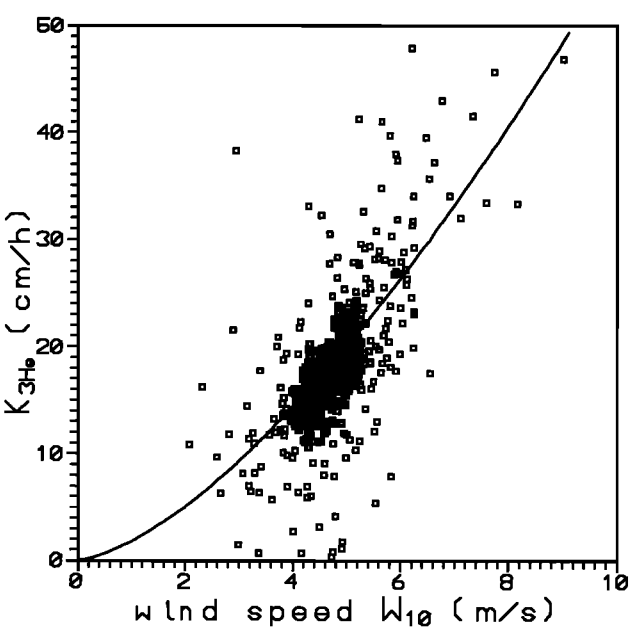

Figure 12. Same as Figure 7a, but using the vertical diffusion model instead of the well-mixed box model. Note the much larger scatter of the results.

the well-mixed reservoir model. It shows that the fluctuations in the tracer's surface layer concentration have a large effect upon the scatter of the K_{ij}. This marked effect could be a significant cause of discrepancy among the experimental gas exchange coefficients reported in the literature, most of which are indeed based on the use of method 2.

This fact is an additional strong argument in favor of the first method for determining the gas transfer velocity/wind speed relationship (i.e., the use of a prescribed functional form), as it avoids both nonlinearity bias and excessive dispersion caused by the experimental scatter of the data and, more important, by any possible departure (even modest) from the well-mixed reservoir conditions.

4. K_{SF6} - K_{3He} Relationship and Schmidt Number Exponent n

To experimentally determine the Schmidt number exponent in (1), the mean ^{3}He and SF_6 transfer velocities K_{ij} are computed, as in section 3.2, for every possible pair of measurements C_i and C_j at times t_i and t_j using (4). Since SF_6 and ^{3}He were not collected at exactly the same time, the ^{3}He data are extrapolated to the corresponding SF_6 sampling time This extrapolation is done using the transfer velocity versus wind speed relationship of section 3.1, the measured wind speed, and the tracer mass balance equation. Figure 13 shows the relationship between the Schmidt number exponent n in (1) and K_{SF6} . The SF_6 and ^{3}He Schmidt numbers are taken from *King and Saltzman* [1995] and *Jähne et al.* [1987a], respectively. The error bars are derived from the analytical errors in SF_6 and ^{3}He measurements and also from the uncertainty quoted in the literature (±5%) in the determination of the Schmidt numbers. Note that the error ΔK in the transfer coefficient varies as the reciprocal of the time interval (t_i-t_j), so that K_{ij} values calculated from large time intervals are more accurate. The general trend shown in Figure 13 is consistent with our current understanding of gas transfer at water-air interface.

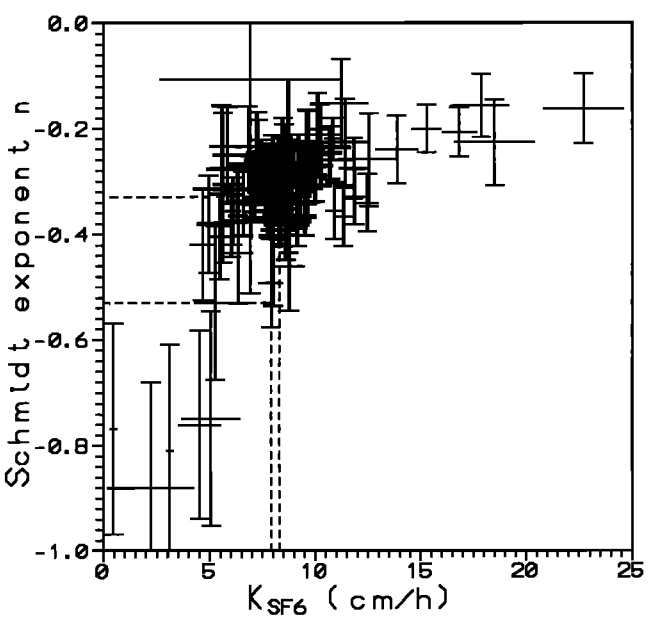

Figure 13. Trend of the Schmidt number exponent versus SF_6 transfer velocity (K_{SF6}) deduced from our experiment. The mean K_{SF6} value for the complete experiment and the average Schmidt number exponent derived from the best fit of the data using $K=\beta W^{1.5}$ are also included (dashed lines).

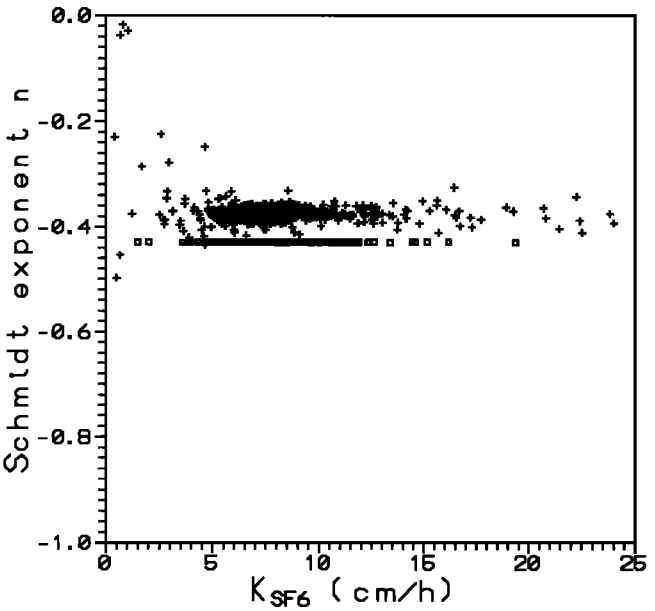

Figure 14. Variation of the Schmidt number exponent versus K_{SF6} using selected pairs on the δ^3He(t) and SF_6(t) best fit curves computed with the well-mixed box model (open squares) and the vertical diffusion model (crosses).

For low transfer regimes, the n exponent is in the range [-1, -2/3] and of the order of -0.5 for intermediate regimes, in agreement with the theory. For higher transfer regimes, however, the value of n keeps increasing and reaches values close to -0.2, possibly owing to the contribution of bubbles to the gas transfer (see discussion below). To check that this trend is not an artifact due to the slight vertical heterogeneity, we compared (Figure 14) the Schmidt number exponent n calculated assuming a well-mixed reservoir (infinite vertical mixing rate) to that calculated for a finite vertical mixing (with D_v=50 cm^2/s). In Figure 14, the squares represent the n values corresponding to all $(K_{ij})_{SF6}$ and $(K_{ij})_{3He}$ pairs determined from fictive δ^3He data points selected at a 1-day frequency on the theoretical curve δ^3He(t) and C_{SF6}(t) of section 3.1 (well-mixed box-model) computed using the power law $K_{3He}=1.8\times W^{1.5}$.and $K_{SF6}=0.71\times W^{1.5}$. The crosses represent the same type of calculation but this time using the vertical diffusion box-model. A comparison between the two sets of results shows that taking into account the vertical heterogeneity shifts the average value of n by 0.05 (-0.38 instead of -0.43) and adds significant scatter to the results. This scatter appears to be greater for low transfer regimes, with a trend to higher n, i.e., the opposite of what is shown in Figure 13. For intermediate- and high- transfer regimes, there is no global effect on the trend of the n exponent versus the transfer regime. This strongly suggests that the experimental trend between n and K_{SF6} observed in our experiment (Figure 13) is not an artifact due to the finite rate of vertical mixing but a genuine phenomenon.

This experimental result supports earlier data of *Wanninkhof et al.* [1993] which show an increase in the apparent Schmidt number exponent with increasing transfer regime (that is, it becomes less negative). Beyond the n=-0.5 value predicted by the models, this increasing trend was interpreted by the authors as the contribution of bubbles to the gas transfer. In this case, the transfer coefficient K'_i for a gas i at any given wind speed can be rewritten as the sum of two components K_i and K_{bi}.

$$K'_i = K_i + K_{bi} \tag{7}$$

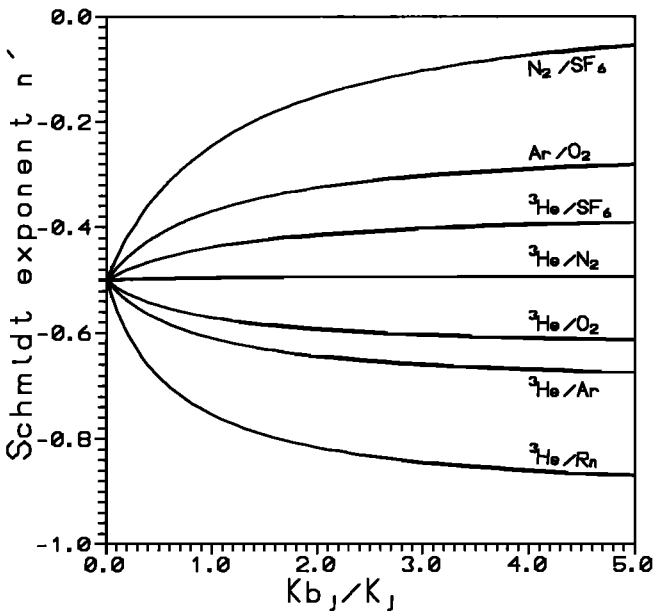

Figure 15. Theoretical variation of the apparent Schmidt number exponent n' versus K_{bj}/K_j derived from equation (8) for various inert gas pairs (i,j). The K_{bi}/K_{bj} ratios have been computed assuming that K_b varies with the gas solubility and diffusivity as $(SRT)^{0.3} D^{0.35}$ (where SRT is the Ostwald solubility coefficient) [*Keeling*, 1993]. Gas solubilities and diffusivities are computed using the polynomial fit of *Wanninkhof* [1992] for freshwater at 8°C.

where K_i is the "normal" gas transfer coefficient and K_{bi} is the contribution due to bubbles. In a dual-tracer experiment, the variable Schmidt number exponent n' which is inferred from the tracer measurements will be linked to the normal n exponent (without gas transfer through bubbles) by the following equation:

$$K'_i/K'_j = (K_i + K_{bi})/(K_j + K_{bj}) = (Sc_i/Sc_j)^{n'} \qquad (8)$$

Giving

$$n' \equiv \frac{\ln[(Sc_i/Sc_j)^n + (K_{bi}/K_{bj})(K_{bj}/K_j)]/(1+K_{bj}/K_j)]}{\ln(Sc_i/Sc_j)} \qquad (9)$$

where K_{bj}/K_j represents the ratio of the bubble-mediated gas transfer to the normal air-sea transfer and K_{bi}/K_{bj} is the ratio of the transfer coefficients through bubbles for the two species. We verify with (9) that if $K_{bj}/K_j \rightarrow 0$ (no bubble contribution to the transfer), then $n' \rightarrow n$, and, on the other hand, if $K_{bj}/K_j \rightarrow \infty$ (gas transfer largely dominated by the bubbles), then $n' \rightarrow \ln(K_{bi}/K_{bj})/\ln(Sc_i/Sc_j)$ (equation (10)). In the general case, (10) shows us that n' values will depend on the relative efficiency of the bubble mediated transfer (K_b/K) of each species i and j and that n' will be larger or smaller than n, depending on the value of the ratio K_{bi}/K_{bj} relative to $(Sc_i/Sc_j)^n$ (Figure 15). Bubble-induced gas exchange in general depends both on the gas diffusivity and solubility, with larger effects for gases with lower solubility [*Merlivat and Memery*, 1983]. *Keeling* [1993] suggested that the bubble-induced gas transfer component K_b should scale as $(SRT)^{0.3} D^{0.35}$ (where SRT is Ostwald solubility coefficient). Because the solubilities of helium and SF_6 are quite similar [*Ashton et al.*, 1968; *Weiss*, 1971], the K_{b3He}/K_{bSF6} ratio will be of the order of $(Sc_{3He}/Sc_{SF6})^{-0.35}$ ($\approx$ 2.13 at 8°C). As this value is below $(Sc_{3He}/Sc_{SF6})^{-0.5}$ ($\approx$ 2.95 at 8°C), the Schmidt number exponent n' should increase relative to n, with an asymptote at n'=-0.35 after (9). This prediction is in apparent agreement with our experimental findings (Figure 13). This agreement could also be fortuitous, however, as it requires a rather large contribution of the bubbles to gas transfer, which is not expected here, considering wind speeds recorded during the experiment. This interpretation of the variation of the Schmidt number exponent based on the influence of bubbles would need to be tested against different gas pairs, especially those with large solubility differences, in order to be fully validated. Therefore the variation of the Schmidt number exponent observed here and its relatively low mean value for the complete experiment are facts, already observed by others (Table 1), whose explanation still requires further clarification.

5-Conclusion

The $SF_6/^3$He deliberately released tracer method in a large freshwater lake of the Kerguelen Islands allowed the determination of both gas transfer velocities in a wind speed range of 0 to 10 m/s, by monitoring SF_6 and ^{3}He escape rates over a month In this experiment, the *Liss and Merlivat* [1986] relationship underestimates the actual gas transfer rate by about 40%. The present results fall in the range of transfer velocities found in most recent experiments [*Wanninkhof et al.*, 1993] and also agree with oceanic $^{14}CO_2$ inventories. Comparison of K_{SF6} and K_{3He} shows, as expected, an increasing trend of the Schmidt number exponent (that is, it becomes less negative) with increasing transfer velocities, but with values extending beyond the n = -0.5 coefficient usually employed for normalizing gas transfer data to CO_2. This raises the problem, discussed previously by different authors and still open to question, of the validity of the normalization methods used to calculate K_{CO2} from gas transfer experiments, especially in high-wind regimes, and points to the need for further clarification of the Schmidt relationship in gas transfer experiments.

Acknowledgements. The KERLAC project was supported by the Territoires des Terres Australes et Antarctiques Françaises (TAAF). We are deeply grateful to A. Lamalle, who supervised with great professionalism the logistics of the project on the Kerguelen Islands. We thank C. Brunet and P. Hegesippe, who took part in the lake survey, and A. L'Huillier and C. Lemarchand, who actively participated in the Suisse Lake experiment.

References

Ashton, J. T., R. A. Dawe, K. W. Miller, E.B.Smith, and B.J.Stickings, The solubility of certain gaseous compounds in water, J. *Chem. Soc., A*, 1793-1796, 1968.

Broecker, W. S., and T. H. Peng, The vertical distribution of Radon in the Bomex area, *Earth Planet. Sci. Lett., 11*, 99-108, 1971.

Broecker, W. S., and T. H. Peng, *Tracers in the Sea*, 690 pp., Lamont-Doherty Earth Observatory, Palisades, N.Y., 1982.

Broecker, W. S., T. H. Peng, G. Mathieu, R. Hesllein and T. Torgersen, Gas exchange rate measurements in natural systems, *Radiocarbon, 22*, 676-683, 1980.

Broecker, W. S., T. H. Peng, G. Ostlund and M. Stuiver, The distribution of bomb radiocarbon in the ocean, *J. Geophys. Res., 90*, 6953-6970, 1985.

Cember, R., Bomb radiocarbon in the Red Sea: a medium-scale gas exchange experiment, *J. Geophys. Res., 94*, 2111-2123, 1989.

Clark, J. F., P. Schlosser, R. Wanninkhof, H. J. Simpson, W. S. F. Schuster, and D. T. Ho, Gas transfer velocities for SF_6 and ^{3}He in a small pond at low wind speeds, *Geophys. Res. Lett., 22*, 93-96, 1995.

Dawson, D. A., and O. Trass, Mass transfer at rough surfaces, *Int. J. Heat Mass Transfer, 15*,1317-1336, 1972.

Deacon, E. L., Gas transfer to and across an air-water interface, *Tellus, 29*, 363-374, 1977.

Emerson, S., W. S. Broecker, and D. W. Schindler, Gas-exchange rate in a small lake as determined by the Radon method, *J. Fish. Res. Board Can., 30*, 1475-1484, 1973.

Gilliland, E. R., and T. K. Sherwood, Diffusion of vapors into air streams, *Ind. Eng. Chem., 26*, 516-523, 1934.

Glover, D. M., and W. S. Reeburgh, Radon-222 and Radium-226 in southeastern Bering Sea shelf waters and sediment, *Cont. Shelf Res., 5*, 433-456, 1987.

Higbie, R., The rate of absorption of a pure into a still liquid during short periods of exposure, *Trans. Am. Inst. Chem. Eng., 35*, 365-369, 1935.

Hutchinson, M. H., and T. K. Sherwood, Liquid film in gas absorption, *Ind. Eng. Chem., 29*, 836-840, 1937.

Jähne, B., K. O. Munnich, and U. Siegenthaler, Measurements of gas exchange and momentum transfer in a circular wind-water tunnel, *Tellus, 31*, 321-329, 1979.

Jähne, B., K. H. Fischer, J. Ilmberger, P. Libner, W. Weiss, D. Imboden, U. Lemnin, and J. M. Jaquet, Parametrization of air/lake gas exchange, in *Gas Transfer at Water Surfaces*, edited by W. Brutsaert and G. H. Jirka, pp. 459-466, D. Reidel, Norwell, Mass., 1984a.

Jähne, B., W. Huber, A. Dutzi, T. Wais, and J. Ilmberger, Wind/wave-tunnel experiment on the Schmidt number and wave field dependence of air/water gas exchange, in *Gas Transfer at Water Surfaces*, edited by W. Brutsaert and G. H. Jirka, pp. 303-309, D. Reidel, Norwell, Mass., 1984b.

Jähne, B., G. Heinz, and W. Dietrich, Measurement of diffusion coefficients of sparingly soluble gases in water with a modified Barrer method, *J. Geophys. Res., 92*, 10,767-10,776, 1987a.

Jähne, B., K., O. Munnich, R. Bosinger, A. Dutzi, W. Huber, and P. Libner, On parameters influencing air-water gas exchange, *J. Geophys. Res., 92*, 1937-1949, 1987b.

Jean-Baptiste, P., F. Mantisi, A. Dapoigny, and M. Stievenard, Design and performance of a mass spectrometric facility for measuring helium isotopes in natural waters and for low-level tritium determination by the ^{3}He ingrowth method, *Appl. Radiat. Isot., 43*, 881-891, 1992.

Keeling, R F., On the role of large bubbles in the air-sea exchange and supersaturation in the ocean, *J. Mar. Res., 51*, 237-271, 1993.

King, D. B., and E. S. Saltzman, Measurement of the diffusion coefficient of sulfur hexafluoride in water, *J. Geophys. Res., 100*, 7083-7088, 1995.

Kromer, B., and W. Roether, Field measurements of air-sea gas exchange by the Radon deficit method during JASIN 1978 and FGGE 1979, *Meteor Forschungergeb., A/B, 24*, 55-75, 1983.

Large, W. P., and S. Pond, Open ocean momentum flux measurements in moderate to strong winds, *J. Phys. Oceanogr., 11*, 324-336, 1981.

Ledwell, J. J., The variation of the gas transfer coefficient with molecular diffusivity, in *Gas Transfer at Water Surfaces*, edited by W. Brutsaert and G. H. Jirka, pp. 293-302, D. Reidel, Norwell, Mass., 1984.

Liss, P. S., and L. Merlivat, Air-sea gas exchange rates: introduction and synthesis, in *The Role of Air-Sea Exchange in Geochemical Cycling*, edited by P. Buat-Menard, pp. 113-127, D. Reidel, Norwell, Mass., 1986.

Merlivat, L., and L. Memery, Gas exchange across an air-water interface: experimental results and modeling of bubble contribution to transfer. *J. Geophys. Res., 88*, 707-724, 1983.

Peng, T. H., T. Takahashi, and W. S. Broecker, Surface Radon measurements in the north Pacific ocean station Papa, *J. Geophys. Res., 79*, 1772-1780, 1974.

Peng, T. H., W S. Broecker, G. G. Mathieu, and Y. H. Li, Radon evasion rates in the Atlantic and Pacific oceans as determined during the Geosecs program, *J. Geophys. Res, 84*, 2471-2486, 1979

Poisson, A., C. Brunet, and P. Hegesippe, Le lac Suisse, archipel des iles Kerguelen: Bathymétrie et hydrologie, report, 55 pp., Terres Austr. et Antarct. Fr., Paris, 1990.

Shaw, D. A., and T. J. Hanratty, Turbulent mass transfer rates to a wall for large Schmidt numbers, *AIChE J., 23*, 28-37, 1977.

Sherwood, T. K., and F. A. Holloway, Performance of packed towers-liquid film data for several packings, *Trans. Am. Inst. Chem. Eng., 36*, 39-70, 1940.

Smethie, W. M., T T. Takahashi, D. W. Chipman, and J. R. Ledwell, Gas exchange and CO_2 flux in the tropical Atlantic Ocean determined from ^{222}Rn and pCO_2 measurements, *J. Geophys. Res., 90*, 7005-7022, 1985.

Top, Z., W. C. Eismont, and W. B. Clarke, Helium isotope effect and solubility of helium and neon in distilled water and seawater, *Deep - Sea Res., Part A, 34*, 1139-1148, 1987.

Torgersen, T., G. Mathieu, R. H. Hesslein, and W. S. Broecker, Gas exchange dependency on diffusion coefficient: direct ^{222}Rn and ^{3}He comparisons in a small lake, *J. Geophys. Res., 87*, 546-556, 1982.

Upstill-Goddard, R. C., A. J. Watson, P. Liss, and M. I. Liddicoat, Gas transfer velocities in lakes measured with SF_6, *Tellus, ser. B, 42*, 364-377, 1990.

Wanninkhof, R., Relationship between wind speed and gas exchange over the ocean, *J. Geophys. Res., 97*, 7373-7382, 1992.

Wanninkhof, R , J. R. Ledwell, and W. S. Broecker, Gas exchange-Wind speed relation measured with sulfur hexafluoride on a lake, *Science, 227*, 1224-1226, 1985.

Wanninkhof, R., J. R. Ledwell, and W. S. Broecker, Gas exchange on Mono Lake and Crowley Lake, California, *J. Geophys. Res., 92*, 14,567-14,580, 1987.

Wanninkhof, R., J. R. Ledwell, and A. J. Watson, Analysis of sulfur hexafluoride in seawater, *J. Geophys. Res., 96*, 8733-8740, 1991a.

Wanninkhof, R., J. R. Ledwell, and J. Crucius, Gas transfer velocities on lakes measured with sulfur hexafluoride, in *Proceedings of the Second International Symposium on Gas Transfer at Water Surfaces*, edited by S. C. Wilhems and J. S. Gulliver, pp. 441-458, Am. Soc. of Civil Eng., New York, 1991b.

Wanninkhof, R., W. Asher, R. Weppernig, H. Chen, P. Schlosser, C. Langdon, and R. Sambrotto, Gas transfer experiment on Georges Bank using two volatile deliberate tracers, *J. Geophys. Res., 98*, 20,237-20,248, 1993

Watson, A. J., R. C. Upstill-Goddard, and P. S. Liss, Air-sea gas exchange in rough and stormy seas measured by a dual-tracer technique, *Nature, 349*, 145-147, 1991.

Weiss, R. F., Helium isotope effect in solution in water and seawater, *Science, 168*, 247-248, 1970.

Weiss, R. F., Solubility of helium and neon in water and seawater, *J. Chem. Eng. Data, 16*, 235-241, 1971.

Whitman, W. G , The two-film theory of gas absorption, *Chem. Metal. Eng., 29*, 146-148, 1923.

P. Jean-Baptiste, Laboratoire des Sciences du Climat et de l'Environnement, CEA/CNRS, Centre d'études de Saclay, F-91191 Gif-sur-Yvette Cedex, France. (pjb@lsce.saclay.cea.fr)

A Poisson, Laboratoire de Physique et Chimie Marines, CNRS/UPMC, 4 place Jussieu, boîte 134, F-75252 Paris Cedex 05, France

(Received June 17, 1996; revised October 28, 1998; accepted January 2, 1999).